5426–5437 *Nucleic Acids Research, 2006, Vol. 34, No. 19* *Published online 29 September 2006*
doi:10.1093/nar/gkl678

SIR2 modifies histone H4-K16 acetylation and affects superhelicity in the ARS region of plasmid chromatin in *Saccharomyces cerevisiae*

Francesco Chiani, Francesca Di Felice and Giorgio Camilloni[1,*]

Dipartimento di Genetica e Biologia Molecolare, Università di Roma 'La Sapienza', Rome, Italy and [1]Istituto di Biologia e Patologia Molecolari, CNR, Rome, Italy

Received March 23, 2006; Revised April 6, 2006; Accepted September 5, 2006

ABSTRACT

The null mutation of the *SIR2* gene in *Saccharomyces cerevisiae* has been associated with a series of different phenotypes including loss of transcriptional silencing, genome instability and replicative aging. Thus, the *SIR2* gene product is an important constituent of the yeast cell. *SIR2* orthologues and paralogues have been discovered in organisms ranging from bacteria to man, underscoring the pivotal role of this protein. Here we report that a plasmid introduced into *sir2*Δ cells accumulates more negative supercoils compared to the same plasmid introduced into wild-type (WT) cells. This effect appears to be directly related to *SIR2* expression as shown by the reduction of negative supercoiling when *SIR2* is overexpressed, and does not depend on the number or positioning of nucleosomes on plasmids. Our results indicate that this new phenotype is due to the lack of Sir2p histone deacetylase activity in the *sir2*Δ strain, because only the H4-K16 residue of the histone octamer undergoes an alteration of its acetylation state. A model proposing interference with the replication machinery is discussed.

INTRODUCTION

In *Saccharomyces cerevisiae,* the dosage and expression level of the *SIR2* gene has been implicated in the regulation of important processes, such as transcriptional silencing, genome stability, DNA repair, chromatin structure and cellular aging (1). Sir2p is a NAD-dependent histone deacetylase (2–4), suggesting that its role in transcriptional silencing might be enzymatic. In addition, Sir2p can perform a weak ADP-ribosylation reaction using NAD as the donor of an ADP-ribose moiety (5,6). Further evidence for the importance of this protein comes from the discovery of the 'sirtuin' protein family, which is conserved from bacteria to humans. Sirtuins are also involved in cell cycle progression, chromosome stability and aging (7,8). Four proteins, designated homologues of sir two (HST), have also been found in *S.cerevisiae* (9).

To carry out its role in transcriptional silencing, Sir2p acts together with three additional silent information proteins, Sir1p, Sir3p and Sir4p (10). Depending on the specific region where silencing occurs, Sir2p cooperates with different partners. In association with Sir1p, Sir3p and Sir4p, Sir2p mediates the silencing at the mating type loci (HML and HMR) (10), while in association with Sir3p and Sir4p it is involved in telomeric silencing. The rDNA is a third genetic locus where transcriptional silencing occurs in *S.cerevisiae*. Here, Sir2p is the only Sir protein necessary for maintenance of the silenced state. At this locus, however, it requires the presence of Net1p (part of the RENT complex) (11,12), which is believed to be crucial for nucleolar localization.

In a *sir2*Δ yeast strain, loss of transcriptional silencing is observed at the rDNA locus; this mutant is also characterized by hyper-accessible chromatin (13,14), hyper-recombination of ribosomal repeat units (15), and decreased life span associated with the accumulation of extrachromosomal circles (ERCs) (16).

In addition, several lines of evidences link *SIR2* to DNA replication. At the rDNA locus of *S.cerevisiae*, it has been reported that Sir2p is preferentially associated with non-replicating chromatin, exerting a form of negative control over origin firing (17); more recently, an additional report has shown that Sir2p negatively controls pre-replication complex (RC) formation by interfering with loading of the MCM complex on the replication origin (18).

Some of the phenotypes associated with the *sir2*Δ mutation are potentially related to DNA supercoiling, an aspect of DNA organization. In particular, similar phenotypes have been reported for *sir2*Δ and *top1*Δ, such as hyper-recombination of rDNA repeat units (15,19), loss of transcriptional silencing at the rDNA locus (20,21) and alteration of histone acetylation (14,22). Since DNA topoisomerase I controls DNA superhelicity, we decided to investigate whether Sir2p may also interfere with the process of supercoiling.

*To whom correspondence should be addressed. Tel: +390649912808; Fax: +390649912500; Email: giorgio.camilloni@uniroma1.it

In eukaryotic cells, DNA superhelicity arises mainly from the wrapping of DNA around nucleosome particles (23), resulting in approximately one negative superhelical turn per nucleosome (24,25). It has been reported that supercoiling of DNA elements (plasmids or excised DNA circles) containing silencer sequences is altered in mutants that affect transcriptional silencing (26–29). Moreover, changing the histone acetylation level has been reported to affect DNA supercoiling (30,31). By analogy, the reported alteration of chromatin structure (13,14) could lead to modification of DNA topology.

MATERIALS AND METHODS

Yeast strains, plasmids and culture media

Strains: W303-1a (Mata, ade 2-1, ura 3-1, his 3-11,15, trp1-1, leu 2-3112, can1-100); Y1422 (sir2Δ) (Mata, leu2-3112, ura3-52, ade8, trp1 Δ901 SIR2:: TRP1) kindly provided by J. Broach; AYH2.45 (Mata, ade2-101, his3-Δ200, leu2-3,-112, lys2-801, trp1-Δ901, ura3-52, adh4::URA3TelVII-L; STY30 (sir2Δ) isogenic to AYH2.45, sir2::TRP1; STY36 (sir4Δ) isogenic to AYH2.45, sir4::TRP1; LJY912 (Mata, ade2-101, his3-Δ200, leu2-3,-112, lys2-801, trp1-Δ901, ura3-52, thr tyr arg4-1, hhf1::HIS3; hhf2::HIS4/pLJ912(CEN3, ARS1, URA3, hhf2 K16Q) and its isogenic PKY501 (Mata, ade2-101, his3-Δ200, leu2-3,-112, lys2-801, trp1-Δ901, ura3-52, thr tyr arg4-1, hhf1::HIS3; hhf2::HIS4/pPK301 (CEN3, ARS1, URA3, HHF2) kindly provided by M. Grunstein. JRY4602(sir3Δ)(Mata, can1-100, his3-11, leu2-3112, lys2Δ, trp1-1, ura3-1, ^GAL sir3Δ::HIS3) kindly provided by Jasper Rine; YKL52 (Mcm7-td) (Mata, ade2-1, ura3-1, his3-11, 15 trp1-1, leu2-3112 can 1-100, MCM7::GAL-Ubiquitin-M-lac1 fragment-Myc-UBR1 (URA3) kindly provided by J. Diffley; WY69 (net1Δ): (Mata, ade 2-1, ura 3-1, his 3-11,15, trp1-1, leu 2-3112, can1-100, net1::HIS5) kindly provided by D. Moazed. AEY1958 (MATα HMRa-e** hht1-hhf1Δ::LEU2 hht2-hhf2Δ::HIS3 pRS414-[HHT1-HHF1]) and AEY1956 (MATα HMRa-e** hht1-hhf1Δ::LEU2 hht2-hhf2Δ::HIS3 pRS414-[HHT1 hhf1-21 (K16R)] kindly provided by A. E. Ehrenhofer-Murray.

YNZ1 (produced in this work) isogenic to PKY501*, sir2::kanMX;* YNZ2 (produced in this work) as LJY912*, sir2:kanMX*.

Plasmids: ypGM1 (32); pRS316 (33), p415Gal, p414Gal (34), pADH426 (35), yCp50 (36), pAR44 (37), pPK301 and pLJ912 (38).

Culture media and conditions

The culture media utilized for cell growth were complete YPD or minimal YNB (39), both supplemented with 2% glucose, or complete YPGal supplemented with 2% galactose when appropriate (see text).

Over-expression of Sir2p was achieved by transforming W303-1a with high-copy number plasmid pAR44 carrying the coding region for Sir2p under the GAL10 promoter as described (37).

Production of YNZ1 and YNZ2 mutants

Standard procedures (40) for SIR2 gene disruption have been employed utilizing the following oligonucleotides (5′–3′): TCGGTAGACACATTCAAACCATTTTTCCCTCATCGGCACATTAAAGCTGGCGGATCCCCGGGTTAATTAA (forward); GGCACTTTTAAATTATTAAATTGCCTTCTACTTAGAGGGTTTTGGGATGTGAATTCGAGCTCGTTTAAAC (reverse).

Induction of Mcm7p degradation

Asynchronous cultures of *mcm7-td UBR1+* and *mcm7-td ubr1Δ ::GAL-UBR1* strains were grown in YP + Glucose medium (GAL-UBR1 OFF) or YP + Galactose (GAL-UBR1 ON) at 24°C. Cells were then shifted to 37°C and samples were taken after 1 h to purify plasmid DNA.

Enzymes and chemicals

Restriction enzymes and micrococcal nuclease were purchased from Roche; *Taq* polymerase from Perkin–Helmer; zymolyase from Seikagaku (Tokyo, Japan); nystatin from Sigma and radiochemicals from Amersham.

Chromatin analysis

Micrococcal nuclease treatment: cells (100–200 ml grown to 0.4 OD/ml) were pelleted and resuspended in 10 ml of a buffer containing 1 M sorbitol, 50 mM Tris–HCl (pH 7.5), 10 mM β-mercaptoethanol, in the presence of 0.03 mg/3×10^7 cells of Zymolyase 100T, and incubated for 10 min at 30°C. The resulting spheroplasts were harvested, resuspended in Nystatin buffer [50 mM NaCl, 1.5 mM $CaCl_2$, 20 mM Tris–HCl (pH 8.0), 0.9 M sorbitol and 100 μg/ml nystatin] (41) and divided into 0.4 ml aliquots. MNase (0.2, 0.4, 0.8 and 1.6 U) was added to each aliquot and the samples were incubated at 37°C for 15 min. The reaction was stopped with 1% SDS, 5 mM EDTA (final concentrations). Proteinase K (40 μg/sample) was added and the samples kept at 56°C for 2 h. The DNA was then purified by three phenol/chloroform extractions and ethanol precipitation. RNase treatment was also performed.

Nucleosome spacing analysis

After MNase treatments and DNA purification the samples were electrophoresed in 1.2% agarose gels (1.75 V/cm), transferred onto a BA-S 85 nitrocellulose membrane (Schleicher & Schuell), hybridized to specific probes according to standard procedures, and detected by autoradiography.

Plasmid purification and 2D electrophoresis

The preparation of circular DNA from yeast cells was performed by alkaline lysis of spheroplasts as reported previously (42). Briefly, cells were treated with Zymolyase as reported for chromatin preparations (see above). Two volumes of 0.2 N NaOH, 1% SDS were added to spheroplasts and the mixture was kept on ice for 10 min; 1.5 vol of 3 M Potassium Acetate (pH 4.8) were then added and the mixture kept on ice for 45 min. After centrifugation, 2 vol of ethanol were added to the supernatant in order to precipitate the circular DNA forms.

2D agarose gel electrophoresis: 2D topoisomer analysis was performed essentially as described by Peck and Wang (43). The plasmid DNA prepared as above, was loaded on 1% agarose gel. The gel was run for 21 h at 60 V in one direction, in cloroquine buffer (30 mM NaH2PO4, 36 mM

Tris, 0.5 mM Na-EDTA and 10 μg/ml cloroquine); afterwards the gel was shaken with 30 μg/ml chloroquine in the same buffer for 2 h, and run in the perpendicular direction for another 16 h in the same buffer at 40 V. The gel was run at room temperature (22°C), with recirculating buffer. Finally, the gel was blotted and hybridized with the specified probe (see text).

To demonstrate that the method employed for plasmids purification does not introduce any artifactual consequences of DNA isolation, we performed the following control. During the DNA purification procedure two samples from WT strain were processed with solutions containing or not 0.1 μg/ml of EtBr. If any nicking closing activity occurs during the purification procedures, the final distribution of topoisomers must be different between the DNA samples prepared in the presence of the intercalator or not. In fact, according to the Fuller equation $L = T + W$, the T-value in a solution containing the EtBr is different from that without EtBr; as a consequence the equilibrium between L and T will be different and the final topoisomer distribution will not be the same between the two samples. No difference is observed between the distribution of DNA samples purified with or without EtBr, demonstrating the absence of DNA topoisomerase activity (or any linking number variation) during the purification procedures (data not shown).

Quantitative evaluation of topoisomer distribution

The digitized images of the films derived from the autoradiography of 2D electrophoresis, were treated as follows: the collective signal of each arc distribution of topoisomers was measured and divided into two parts: one consisting of the negative topoisomers and the other of the positive ones. The same treatment was employed for all the samples analyzed by the 2D gel electrophoresis. The two values of the arch representing negative and positive topoisomers were reported as percentage of the total signal in the arch. Percentage distribution of negative topoisomers was then normalized to that of WT. The resulting value was considered as the increase of negative distribution (ind) being >1 for increased negative distribution and <1 for increased positive supercoiling.

Chromatin immunoprecipitation (ChIP)

A total of 100 ml of culture were grown to exponential phase (0.4 OD/ml), formaldehyde-fixed and processed for ChIP as described (44,45). DNA was sheared by sonication to an average size of 500–800 bp in all experiments. Chromatin was immunoprecipitated with antibody against acetylated Lys9 or Lys14 of H3 and Lys16 of histone H4 (Upstate Biotechnology). Chromatin–antibody complex was isolated with Protein A Sepharose Beads (Amersham). The immunoprecipitated DNA were analyzed by multiple PCR using the following primers: ACT1f: 5′-ACGTTCCAGCCTTCTACGTTTCCA-3′; ACT1r: 5′-AGTCAGTCAAATCTCTACCGGCCA-3′; ARSH4f: 5′-GTCTGTGTAGAAGACCACACACGA-3′; ARSH4r: 5′-TTTCTTAGGACGGATCGCTTGCCT-3′; LINKf: 5′-GTTACATGCGTACACGCGTCTGTA-3′; LINKr: 5′-TCAAGCTTATCGATACCGTCGACC-3′; TEL IVf: 5′-GCGTAACAAAGCCATATTGCCTCC-3′; TEL IVr: 5′-CTCGTTAGGATCACGTTCGAATCC-3′. [α-^{32}P]dATP was added to the reaction (0.5 μCi/12.5 μl). Quantitation was performed using a PhosphorImager.

Probes

The following probes have been utilized in this work: probe AMP deriving from PCR amplification of 5′-CAGTCTATTAATTGTTGCCGG-3′; 5′-AGTGCTGCCATAACCATGAGT-3′ and corresponding to the beta-lactamase region (from 238 to 487 nt of the coding sequence of beta-lactamase gene) of all plasmids utilized.

Probe LINK derives from restriction of pRS316 by PvuII. The fragment containing the polylinker was then digested with EcoRI and purified.

RESULTS

SIR2-dependent alteration of plasmid topology

It has been demonstrated that yeast plasmids or DNA regions containing silencer elements become altered in their topology when excised from their chromosomal contexts (26–29). These topological alterations are dependent on the *SIR2-4* genes.

We evaluated whether a segment of rDNA inserted into a yeast shuttle vector could behave like the silencer elements reported previously. In addition, to determine whether rDNA could attract Sir2p (as do silencers) and affect DNA topology, we studied a yeast plasmid derived from pRS316, in which a portion of the NTS sequence of the rDNA locus was cloned, yielding the ypGM1 plasmid described previously (14); in fact, it has been reported that Sir2p interacts with the NTS region of rDNA in its chromosomal context (46), although no specific silencer has been detected in this region. We compared WT and *sir2*Δ strains (lacking the only gene involved in all known types of transcriptional silencing in *S.cerevisiae*) transformed with ypGM1.

Cells transformed with ypGM1 or with the original vector plasmid (see below) were grown in minimal media to exponential phase (0.4 OD/ml). Plasmids were then purified as described previously (42) and DNA topoisomers were resolved by 2D agarose gel electrophoresis in the presence of different amounts of the intercalator cloroquine in orthogonal directions. This procedure (43) allows high resolution of different topological DNA forms, resulting in a scattered distribution along an arc of positive (more rightward) and negative (more leftward) topoisomers. The distributed DNA topoisomers were then transferred onto a nitrocellulose filter and hybridized to a labeled probe (the linearized plasmid itself).

When ypGM1 was analyzed by 2D electrophoresis, we observed (Figure 1A) that the distribution of topoisomers from the *sir2*Δ strain was more negatively supercoiled compared to the one from the WT strain (note the leftward shift of the arc in *sir2*Δ compared to WT). When the topoisomer distribution was analyzed by densitometric scanning, we observed that in the sir2Δ strain, the increase of negative distribution (ind) was 1.8 times greater than in WT (each distribution is compared with the WT, assigned the standard value of 1); this value was calculated as described in the Materials and Methods section. In order to determine whether this effect was due to the presence of the NTS sequence in the

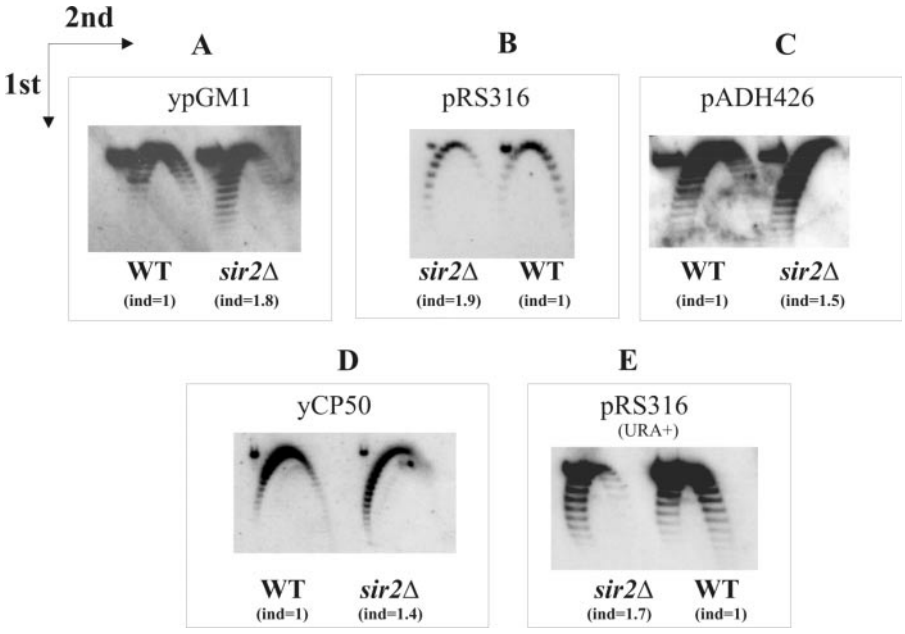

Figure 1. Analysis of the topoisomer distribution in different yeast plasmids in WT and *sir2*Δ cells. WT or *sir2*Δ cells, transformed with the specified plasmid (indicated in each square) were grown to exponential phase and circular DNA purified. 2D electrophoresis was then performed with two different concentrations of cloroquine: 10 and 30 μg/ml in the first and second dimension, respectively. After electrophoresis, DNA samples were transferred to a nitrocellulose filter and hybridized with the probes specified. The topoisomers are distributed along an arc-shaped trajectory. Negatively and positively supercoiled topoisomers are found in the left and right parts of the arc, respectively. Each square marked by a capital letter (**A**–**E**) shows a comparison between WT and *sir2*Δ strains for the specified plasmid. (B and E) show the same plasmid in WT and *sir2*Δ strains in the absence (A) or presence (E) of uracil in the growth medium. The ind values reported at the bottom of each topoisomer distribution indicate the increase of negative distribution evaluated by densitometric analysis.

plasmid, we extended our analysis to the vector alone (pRS316 without a specific insertion). In this case also, the distribution of DNA topoisomers from *sir2*Δ cells was more biased towards negative supercoiling than in WT cells, as shown in Figure 1B. As both ypGM1 and pRS316 contain a CEN6 and an ARSH4 replication origin, it is perhaps not surprising that the ind values in particular are very similar. In order to assess the influence of the centromere and replication origin sequences, we used a non-centromeric plasmid containing the 2 μ replication origin, pADH426 (35). In this case we also observed (Figure 1C) results similar to those reported for the plasmids just described with an ind value of 1.5. A more negatively supercoiled distribution of topoisomers in *sir2*Δ versus WT was also observed both with the yCP50 plasmid (36) carrying a different replication origin (ARS1) and a different centromeric sequence (CEN4 instead of CEN6) (Figure 1D), and with the p414GAL (34), Figure 5 (compare WT and *sir2*Δ samples) differing in the selectable marker (*TRP1* instead of *URA3* present in all the previous plasmids). Further evaluation of the selectable marker influence on plasmid topology has been performed on a *LEU2* based plasmid (p415Gal) and a coherent result was obtained (data not shown). In all the plasmids so far studied, the alteration of DNA topology depends on the *SIR2* gene but is independent of the presence of specific elements, such as ribosomal sequences, selectable markers, centromeres or replication origins. The increase in negative superhelical distribution for different plasmids ranged from 1.9- to 1.3-fold relative to WT.

To ascertain whether ongoing transcription of the selectable marker (present on all the plasmids analyzed) was important for the topological shift observed [according to the twin domain model (47)], we analyzed the distribution of topoisomers for pRS316 (48) bearing *URA3* as selectable marker, from cells grown in synthetic media containing or lacking uracil. In fact, the *URA3* gene can be down-regulated several-fold by the presence of uracil (49). As reported in Figure 1E, the *sir2*Δ dependent effect is still observed in cells grown in the presence of uracil, where the URA3 gene is transcribed at a very low level as evaluated by RT–PCR analysis (data not shown). The alteration seems to be very similar to that observed in medium lacking uracil (Figure 1B). From these data, we can conclude that transcriptional events occurring on the plasmid analyzed do not cause the topological shift observed (more negative distribution of topoisomers), which is thus due solely to the *sir2*Δ mutation. In addition, we observe that the shift in supercoiling distribution decreases with increasing plasmid size, being lower (ind 1.3–1.2) for plasmids larger that 7 kb.

The amount of Sir2p directly correlates with topological alterations

The results shown in Figure 1 demonstrate that in the *sir2*Δ mutant, plasmid DNAs are always more negatively supercoiled than those extracted from WT strains. It is worth emphasizing that the experiments were performed with three different *sir2*Δ strains: Y1422 (50) for the experiments reported in Figure 1A–D; YNZ1 for Figure 5 and STY30 (51) (data not shown). This observation suggests that the alteration

of plasmid supercoiling is indeed mostly due to the lack of Sir2p (by a direct or indirect mechanism) and not to the global genetic background.

In order to verify the hypothesis that Sir2p directly affects the topology of the plasmids, we studied the topological state of the plasmids previously analyzed in strains with *SIR2* placed under heterologous control to allow a different rate of transcription. We transformed WT cells (W303-1A) with the plasmid pAR44 containing the *SIR2* gene under the GAL10 promoter (37); these cells were then transformed with pRS316, grown in minimal medium containing 2% glucose to exponential phase, collected, washed, split in two equal parts and shifted for 2 h to minimal medium with 2% galactose or 2% glucose, in order to either induce or repress *SIR2* gene transcription from the pAR44 plasmid. It is important to emphasize that the pRS316 plasmid on which the topological analysis is performed does not contain any sequence responsive to the presence of galactose. DNA enriched in circular forms was prepared as described above and run on a 2D agarose gel. DNA samples from WT cells transformed with pAR44 (un-induced and induced with galactose) were loaded on the same gel; DNA from *sir2*Δ cells was also loaded as a reference. The DNAs were transferred to a nitrocellulose filter and hybridized to a pRS316 probe (detailed in Materials and Methods). Figure 2A shows the comparison of topoisomer distributions among *sir2*Δ, WT and $SIR2^{++}$ (over-expression) strains. The average distribution shifts from more negative (*sir2*Δ*)* to more positive topological forms ($SIR2^{++}$), correlating with the increase in the level of Sir2p in the cells. Note the arc shape: shifted toward the left in *sir2*Δ cells, centered in WT cells not induced with galactose, and shifted toward the right for DNA from cells induced with galactose to overproduce Sir2p. In this experiment, the ind value ranges from 1.3 (relative to WT) to 0.5. Taken together, these results demonstrate that supercoiling of DNA topoisomers depends on the amount of Sir2p present inside the cells, and that increasing Sir2p moves the distribution toward positive topoisomers (Figure 2A, sample $SIR2^{++}$); the absence of Sir2p produces the opposite result (Figure 2A, sample *sir2*Δ) inducing more negative supercoiling.

Sir4p contributes to the topological influence of Sir2p on plasmid DNA

In *S.cerevisiae* Sir2p is present in two major protein complexes (52,53). One is characterized by the presence of Sir4p and the other by the presence of Net1p. In order to investigate whether Sir2p may affect the distribution of plas-

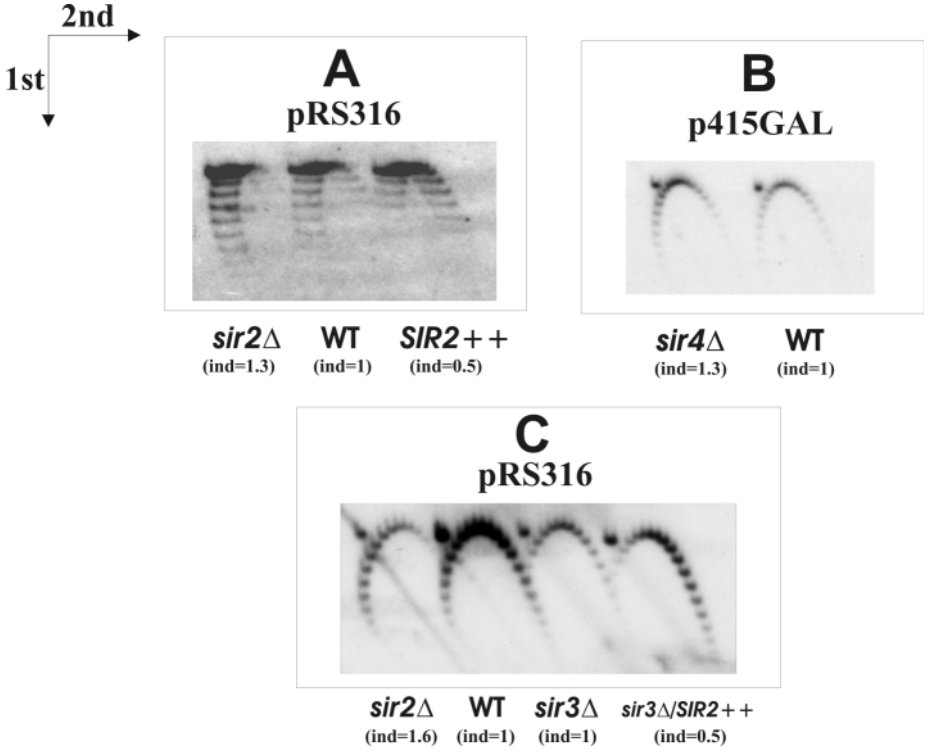

Figure 2. (**A**) Overexpression of the *SIR2* gene leads to positively supercoiled topoisomers. WT cells transformed with pAR44 (carrying the coding region of Sir2p under GAL10 promoter) were induced (Sir2++) or not (WT) with galactose. After a 2 h induction, plasmid DNA was extracted, purified and electrophoresed as reported in Figure 1. The *sir2*Δ sample is included as a reference for negatively supercoiled topoisomers. (**B**) *sir4*Δ behaves like a *sir2*Δ mutant with respect to altering plasmid topology, implicating the SIR2–SIR4 complex. WT and *sir4*Δ cells were transformed with p415GAL, grown to exponential phase and plasmid DNA purified as in Figure 1. DNA samples were subjected to 2D electrophoresis as in Figure 1. Bands outside the arc trajectory represent open circle molecules. The ind values reported at the bottom of each topoisomer distribution indicate the increased negative supercoil distribution evaluated by densitometric analysis. (**C**) Sir3p does not affect plasmid topology. *Sir2*Δ, WT, *sir3*Δ and *sir3*Δ over-expressing Sir2p cells were transformed with pRS316, grown to exponential phase and plasmid DNA purified as in Figure 1. Over-expression of Sir2p in the *sir3*Δ strain, was engineered as for the experiments shown in Figure 1A (sample *sir2*++). DNA samples were subjected to 2D electrophoresis as in Figure 1. Bands outside the arc trajectory represent open circle molecules. The ind values reported at the bottom of each topoisomer distribution indicate the increased negative supercoil distribution evaluated by densitometric analysis.

mid topoisomers through one or the other of these complexes, we compared WT and *sir4*Δ yeast strains, both transformed with p415GAL. In Figure 2B, we report a 2D analysis of plasmid p415GAL from *sir4*Δ or WT cells. A shift of the arc towards more negative supercoiled forms in the plasmid extracted from *sir4*Δ cells is observed. The distribution is identical to that observed when the same plasmid was studied in *sir2*Δ cells (data not shown). Conversely, when WT and *net1*Δ cells were transformed with the pRS316 plasmid, no differences were observed in the distribution of topoisomers after 2D gel electrophoresis (data not shown).

These data demonstrate that the topological shift is dependent on both *SIR2* and *SIR4*, but not on *NET1*, strongly suggesting that Sir2p influences plasmid topology as a member of the complex containing Sir4p.

Sir3p is not involved in alteration of plasmid topology

The involvement of the *SIR3* gene in the alteration of plasmid topology has also been evaluated. We studied the *sir3*Δ mutant in comparison with a WT, a *sir2*Δ and a *sir3*Δ overexpressing Sir2p strain. Figure 2C shows that there is no significant alteration of plasmid topology in the *sir3*Δ mutant compared to WT (samples 1 and 2); in addition the *sir3*Δ overexpressing Sir2p strain behaves like the WT strain overexpressing Sir2p (more positive distribution of topoisomers; see Figure 2A). This implies that Sir3p is not involved in the alteration of plasmid topology, in contrast to what was shown for *sir2*Δ and *sir4*Δ strains.

The results obtained with *sir2*Δ mutants concerning the shift of plasmid topology (Figures 1 and 2) are clearly opposite to those previously obtained when circular DNAs containing silencer elements were studied (26–29); in fact, in those experiments, performed in *sir2*Δ, *sir3*Δ or *sir4*Δ mutants, an increase in positive supercoiling was observed. In addition, *in vitro* results have demonstrated that histone hyperacetylation increases positive supercoiling (30,31). We therefore considered the possibility that the observed alteration of the plasmid topology is not due to altered histone modification throughout the entire plasmid.

Plasmid nucleosome spacing is not affected by the *sir2*Δ mutation

Altering the number of nucleosomes, as well as their distribution or conformation, could influence DNA topology. For this reason, we investigated whether nucleosome spacing on a plasmid was altered in the *sir2*Δ mutant. WT or *sir2*Δ cells transformed with pRS316, grown to exponential phase, were processed for spheroplast formation and permeabilized with nystatin as reported previously (41). The permeabilized spheroplasts were subjected to micrococcal nuclease (MNase) digestion as reported (32). DNA was then purified and loaded on an agarose gel. After electrophoresis, samples were transferred onto a nitrocellulose filter and hybridized to different probes in order to detect the presence of nucleosomes in two major regions of the plasmid. As shown in Figure 3A, when the filter was hybridized to the AMP probe, described previously (for details see Materials and Methods), organization into regularly spaced nucleosomes (closed ellipses in the schematic drawing shown in Figure 3C) involving at least four particles was evident. Since the spacing analysis is not oriented, we can conclude that this organization occurs both at the left and at the right sides of the probe. In addition, no

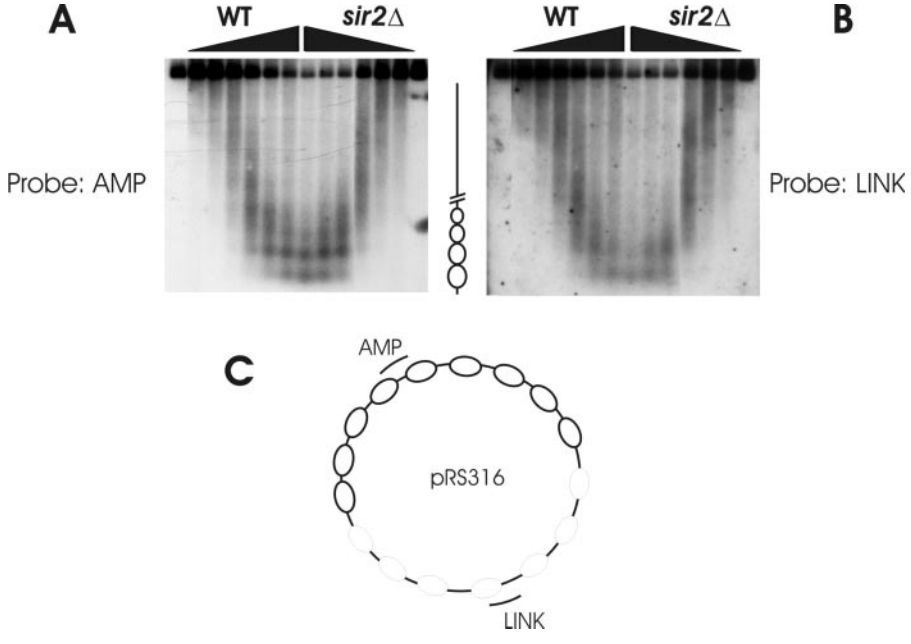

Figure 3. Plasmid chromatin organization does not differ between WT cells and the *sir2*Δ mutant. WT and *sir2*Δ cells transformed with pRS316 were grown to exponential phase and subjected to MNase digestion after permeabilization with nystatin. Afterwards, total DNA was extracted, purified and subjected to agarose gel electrophoresis. DNA fragments were transferred onto a nitrocellulose filter and hybridized to AMP (**A**) or LINK (**B**) probes in order to reveal nucleosome spacing in two different regions of pRS316. Triangles indicate increasing (or decreasing) amounts of MNase used in the assay. The drawing at the bottom of the figure (**C**) describes interpretation of the data. Thick-lined ellipses indicate nucleosomes with a clear spacing profile; dotted-line ellipses indicate nucleosomes with less defined spacing profiles.

differences are detected between the WT and the *sir2*Δ profiles. When the AMP probe was stripped from the filter followed by re-hybridization to the LINK probe (annealing from 1878 to 2001 of the pRS316 sequence) we observed a slightly different profile (Figure 3B). In this case, only 2–3 nucleosomal particles with defined spacing are visible, most likely reflecting a less organized chromatin structure (dotted ellipses in the schematic drawing reported in Figure 3C). However, in this region also we observe no significant differences between the WT and *sir2*Δ profiles. Considering that with this analysis we are able to scan ~2000 nt for each probe and that pRS316 is ~4 kb long, we conclude that there is no dramatic difference in the nucleosome arrangement between WT and *sir2*Δ strains.

Additional experiments, performed by the end-labeling technique (exploring the ARS sequence), did not show either positioned nucleosomes nor differences between the WT and *sir2*Δ strains (data not shown).

The topological alteration of plasmid DNA in *sir2*Δ mutants correlates with specific deacetylation of histone H4 at the K16 residue in the ARS region

Most of the phenotypes shown by *sir2*Δ mutants arise from the lack of histone deacetylase function (8). This enzymatic activity yields hyperacetylated chromatin (54). In order to determine whether the topological alterations we observe are also due to hyperacetylation of plasmid chromatin, we set up ChIP experiments to measure the acetylation level of the histone residues modified by Sir2p on the plasmids studied; we considered two regions in the plasmid analyzed (ARSH4 and polylinker) and also two chromosomal regions as reference (ACT1 and TEL IV). WT and *sir2*Δ cells were grown in minimal medium to exponential phase. After cross-linking with formaldehyde, whole cell extracts were prepared and the DNA–protein samples were immunoprecipitated with specific antibodies [anti-Acetyl-K9(H3), anti-Acetyl-K14(H3) and anti-Acetyl-K16(H4)]; the cross-linking was reversed and the DNA purified. A multiplex PCR was set up, coamplifying with four pairs of primers corresponding to the following sites: (i) the ARSH4 region of the p415GAL plasmid (ARSH4), (ii) the linker region of the p415GAL plasmid (LINK), (iii) the promoter region of ACT1 gene (ACT1) and (iv) the Tel IV subtelomeric region (TEL IV). As shown in Figure 4A, no enrichment was observed for the polylinker and ACT1 regions in the two strains (negative controls) compared to the respective input values (lanes 1–3, INPUT); in the telomeric region (Tel IV), where Sir2p is known to act (51), the acetylated form of all the histone residues studied is strongly enriched (lanes 4–12 in sir2Δ). As far as the ARSH4 region is concerned, we observed that in the sir2Δ strain, the only hyperacetylated residue relative to WT was H4-K16 (lanes 10–12, in sir2Δ). A quantitative representation of the data are shown in Figure 4B, where the ratios of sir2/WT values for each residue studied (normalized to their INPUT) is reported. Taken together, these data demonstrate that in

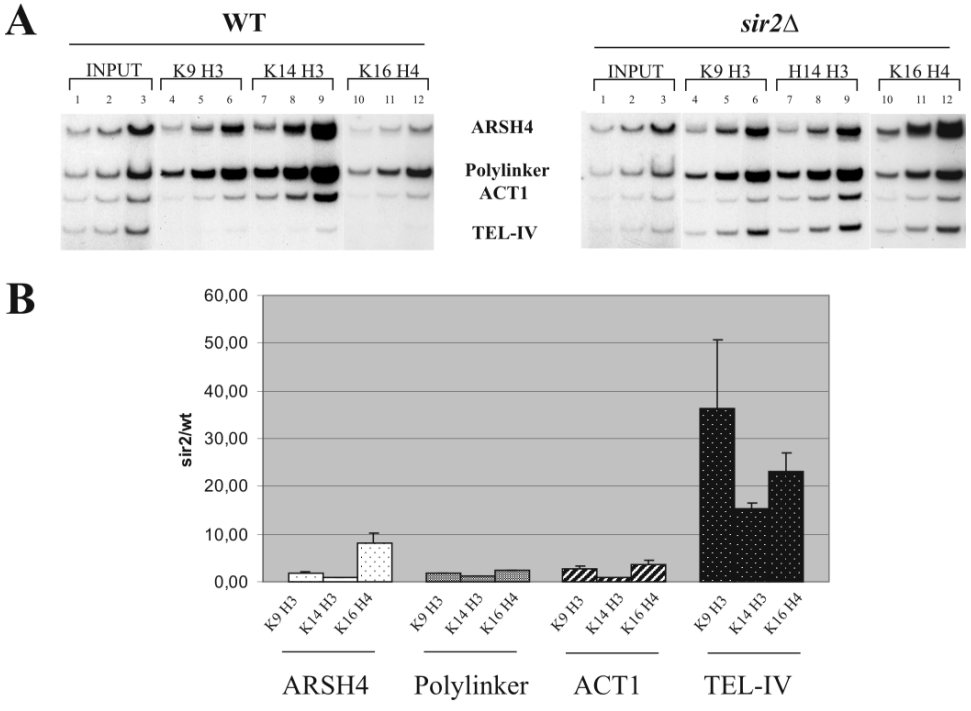

Figure 4. (**A**) The histone deacetylase activity of Sir2p alters acetylation of the H4-K16 residue in the plasmid ARS. WT and *sir2*Δ cells transformed with p415GAL were subjected to the standard treatment for ChIP. Coamplification products of four different DNA regions were reported: ARSH4 refers to a region encompassing the ARSH4 and adjacent plasmid DNA of p415GAL; Link refers to a region encompassing the polylinker of p415GAL; ACT1 refers to the actin gene in its chromosomal location and Tel IV refers to a subtelomeric (telomer IV, L-arm). INPUT (1–3): coamplification of three doubled amounts of samples from whole cell extract (without immunoprecipitation). Samples IP, lanes 4–6: whole cell extract immunoprecipited with anti K9-H3 antibodies and coamplified in three doubled amounts; lanes 7–9 samples as in 4–6 immunoprecipited with anti H3-K14; lanes 10–12, samples as in 4–6 immunoprecipited with anti H4-K16; WT and *sir2*Δ indicate samples treated for ChIP analysis from WT and *sir2*Δ cells. (**B**) Shows a graphic representation comparing the ratio of the *sir2*Δ/WT ratio normalized to relative INPUTS for ARSH4, Polylinker, ACT1 and TEL-IV.

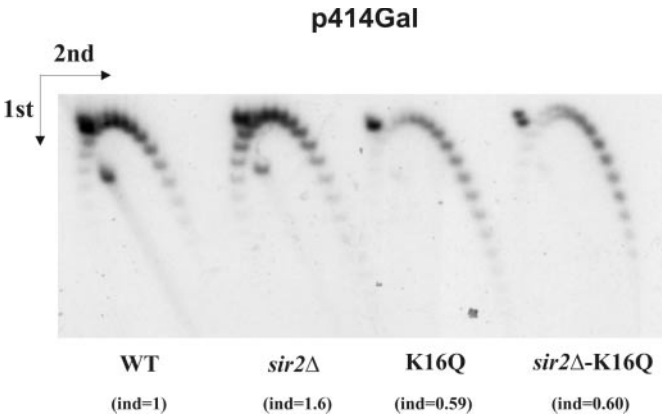

Figure 5. The *sir2*Δ mutant does not alter plasmid supercoiling in a strain carrying a K16Q mutation. WT, *sir2*Δ, K16Q and *sir2*Δ-K16Q cells were transformed with p414Gal. The cells were grown and the plasmids purified and analyzed as in Figure 1. Ind values reported at the bottom of each topoisomer distribution indicate the increased distribution of negative supercoils as evaluated by densitometric analysis.

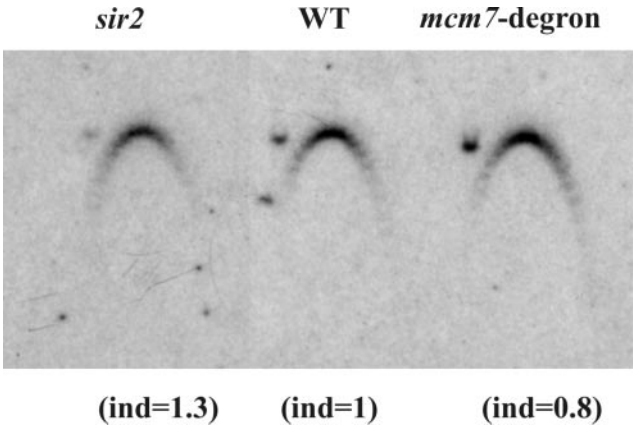

Figure 6. The absence of the MCM complex results in positive supercoiling of the p415GAL plasmid. Cells carrying the *mcm7-td* allele transformed with p415GAL were induced to degrade Mcm7p or not by growth in galactose or glucose medium, respectively. After 1 h of treatment, the plasimd DNA was purified and analyzed as in Figure 1. Plasmid DNA from the *sir2*Δ mutant strain was included as a reference.

the *sir2*Δ mutant, where topological shifts have been observed (Figures 1 and 2), plasmid chromatin is hyperacetylated at H4-K16, suggesting that SIR2-dependent deacetylation of plasmid chromatin may play a role in the alteration of superhelicity.

Mutating K16 to Q16 of histone H4 prevents shift of plasmid supercoiling in the *sir2*Δ background

The data shown in Figure 4 indicate that acetylation of K16 in histone H4 is linked to SIR2-dependent changes in plasmid supercoiling. In order to demonstrate that acetylation of the H4 residue K16 is directly involved in the SIR2-dependent shift of yeast plasmid supercoiling, we compared three different mutant strains and their isogenic WT counterparts with respect to a shift in the p414Gal topology. The mutations analyzed were *sir2*Δ, histone H4 K16 to Q16 and the double mutant carrying both mutations. We produced the *sir2*Δ and the *sir2*Δ, H4K16Q strains by disrupting the SIR2 gene in the K16Q mutant and an isogenic WT strain. If the shift in supercoiling is linked to H4-K16 deacetylation, it should be blocked in the *sir2*ΔK16Q mutant which cannot undergo modification of this residue.

Plasmid analysis reported in Figure 5 (performed as in Figure 1) demonstrates that, relative to the WT background (ind = 1), the K16Q mutation yields a more positive distribution of topoisomers (see K16Q in Figure 5, ind = 0.59). While in a WT context the *sir2*Δ (Figure 5, *sir2*Δ ind = 1.6) mutation yields a more negative distribution of topoisomers (based on the data shown in Figures 1 and 2), no change in supercoiling is observed in the *sir2*ΔK16Q double mutant (ind = 0.60) relative to K16Q (ind = 0.59) alone. This result provides strong evidence that the K16 residue of histone H4 is involved in the *SIR2*-dependent shift in plasmid supercoiling and that the K16Q is dominant over the *sir2*Δ mutation.

mcm7-td mutant cells show increased positive supercoiling of plasmid DNA

Recently, Pappas and colleagues (18) demonstrated that Sir2p interferes with loading of the MCM complex on several ARS sequences, and further showed that the deletion of *SIR2* increases Mcm2p binding to the ARS315 and ARS501 chromosomal origins. We hypothesized that the different efficiency of MCM loading on ARS plasmids could lead to an altered DNA topology. In order to test whether the lack of MCM yields positive supercoiling of plasmid DNA, we studied the *mcm7*-td (temperature-inducible degron) mutant in induced and un-induced conditions. In a *mcm7*-td mutant, the Mcm7-td protein is present when cells are grown at 24°C in the presence of galactose to induce high levels of GAL-UBR1 expression, but is very rapidly degraded upon shifting the cells to 37°C and disappears in ~30 min (55).

mcm7-td cells were transformed with p415GAL and grown to exponential phase at 24°C in minimal medium plus 2% glucose. The cells were then washed and shifted for 1 h to minimal medium plus 2% galactose at 37°C in order to induce the Ubr1p that leads to Mcm7p degradation, or to minimal medium plus 2% glucose where Mcm7p remains intact; Mcm7p disappearance was evaluated by western blot analysis (data not shown). DNA enriched in circular forms from both conditions (induced with galactose and un-induced) were prepared as reported above and run on a 2D agarose gel. Afterwards, samples were transferred to a nitrocellulose filter and hybridized to a p415GAL probe. Figure 6 shows a comparison of the topoisomer distribution between uninduced and induced *mcm7-td* cells. A shift of the distribution of topoisomers is observed between the different samples. The uninduced *mcm7*-td strain is centrally distributed while in the induced *mcm7*-td strain, more positively supercoiled topoisomers are present. Thus, the lack of a functional MCM complex yields an average distribution shifted toward positive topoisomers.

DISCUSSION

SIR2 affects DNA topology by increasing negative supercoiling

In this study, we observed an increase of negative supercoiling of different plasmids when introduced in the *sir2*Δ strain

compared to the WT strain (Figure 1). However all the shifts of plasmid topology observed in this study should be interpreted as an *in vivo* shifts in topoisomer frequency toward higher or lower relative linking number values. In fact the analyses of topological shifts should be interpreted as relative and not absolute. Previous reports described increased positive supercoiling of circular DNA (plasmids or excised rings) containing silencer or telomeric sequences in *sir2*Δ mutants (26–29). We thus hypothesized that the topological shift we observed could be due to a different cause. When different plasmids were assayed for topoisomer distribution, we consistently found an increase in negative supercoils in *sir2*Δ cells compared to WT. The plasmids analyzed were yeast vectors without specific insertions, sharing only the ARS consensus sequence (ACS) (56,57) for DNA replication. Our data indicate that neither the replication origin (ARS1, ARSH4 or 2 μ), the CEN sequence (CEN4 and CEN6), the selectable marker (URA, TRP or LEU) nor active transcription seem to be required for this increase in negative supercoils in *sir2*Δ cells (Figure 1B; Figure 5 WT versus *sir2*Δ). The only noticeable change in the magnitude of the increase occurred when plasmids of different size were compared. This suggests that a limiting factor that acts on plasmid DNA to exert topological modification becomes less effective when the size of the DNA increases.

We then asked whether the level of SIR2 expression could affect the DNA topology. We observed (Figure 2A) that the degree to which Sir2p is overexpressed correlated with the distribution of positive supercoiled topoisomers, suggesting that increasing the amount of Sir2p promotes this phenomenon.

It has been described in *S.cerevisiae* that Sir2p is present in two major particles: the SIR2/4 and the RENT complexes (52,58). Thus, we also evaluated the topoisomer distribution in *sir4*Δ and *net1*Δ mutants, since the products of these genes are considered crucial for association of Sir2p within the Sir2p–Sir4p complex and the RENT complex, respectively (52,58). When plasmid DNA from *sir4*Δ or *net1*Δ mutants was analyzed by 2D gel electrophoresis, we observed that only the *sir4*Δ strain shows the same distribution of negatively supercoiled topoisomers as does *sir2*Δ. Conversely the *net1*Δ mutant shows the same distribution as WT cells; these observations suggest that the shift of DNA topology was due to Sir2p acting in the context of the Sir2p–Sir4p complex.

As far as the *sir3*Δ mutation is concerned, our findings suggest that Sir3p does not affect topoisomer distribution (see Figure 2C), indicating that the observed alteration of plasmid topology depends on the concerted action of the Sir2 and Sir4 proteins only.

Plasmid chromatin organization does not correlate with topological alterations

The wrapping of DNA around histone octamers introduces superhelical turns into plasmid DNA in yeast cells (23). In order to evaluate whether altered chromatin organization occurs in *sir2*Δ cells, we studied nuclesome spacing by MNase digestion of permeabilized spheroplasts. This assay reveals the presence of nucleosomes by producing the 'nucleosomal ladder', with multiple bands typically spaced at ∼200 bp. When the assay was performed on pRS316, we did not observe any difference in the pattern of nucleosomal spacing in plasmid chromatin from WT versus *sir2*Δ strains (Figure 3). Further approaches utilizing the end-labeling method to detect nucleosomes also failed to show differences between the two strains, suggesting that a change in chromatin organization did not account for the topological alterations observed.

The histone deacetylase activity of Sir2p is involved in the alteration of topology

The topological shifts that we observed are not in agreement with previous experiments (26–29) from two points of view: (i) the alteration of supercoiling also occurs in plasmids that do not contain any silencer or telomeric sequences and (ii) the plasmid topology shifts toward negative topoisomers.

In order to explore these differences, we hypothesized that the phenomenon observed is not due directly to the known histone-deacetylase activity of Sir2p in terms of distortion of histone–DNA interactions. Thus, we asked the following question: is the acetylation level of plasmid chromatin altered in a *sir2*Δ mutant? In fact, lack of Sir2p activity would result in hyperacetylated chromatin and it has been demonstrated *in vitro* that hyperacetylated nucleosomal particles yield positive superhelical turns (31). To answer this question, we evaluated the acetylation level of plasmid nucleosomes. We observed an increase of acetylation of only histone H4, specifically the K16 residue, using plasmid by ChIP in the *sir2*Δ mutant (Figure 4). Considering the increased negative supercoiling in *sir2*Δ mutants, and the absence of shift in supercoiling in the *sir2*ΔK16Q double mutant, we conclude that the histone deacetylase activity of Sir2p, particularly on H4-K16, is involved in altering plasmid DNA topology, probably without affecting DNA–histone interactions enough to shift the topological distribution towards positive topoisomers.

In fact, when all the H4 histones of the cells were modified by the mutation of K16 to Q16, mimicking the acetylated state (Figure 5), or K16 to R16 mimicking the deacetylated state (data not shown), a consistent shift toward respectively positive or negative topoisomers is observed; this is in agreement with previous reports (31) where hyperacetylation or hypoacetylation of histones correlates with more positive or more negative topoisomer distribution, respectively. This does not occur when the H4 residue is modified in the only ARS region in the plasmids. We propose that the modified K16 residue in H4 bound in the ARS region could represent a signal required for pre-RC assembly (see below).

Loading of the MCM complex affects DNA topology

An interesting link between *SIR2* and DNA replication has been reported (18). The authors showed that the MCM complex is more efficiently loaded onto several ARS elements when the *sir2*Δ mutation is present. The MCM complex contains a helicase activity (59). We hypothesized that unwinding of DNA coupled with a DNA topoisomerase activity would yield more negative supercoiling in *sir2*Δ cells where more efficient loading of MCM complex occurs. In fact, the absence of Sir2p could induce an increase of helicase activity, with a consequent accumulation of torsional stress on DNA, due to the two strands unwinding. Thus, the DNA

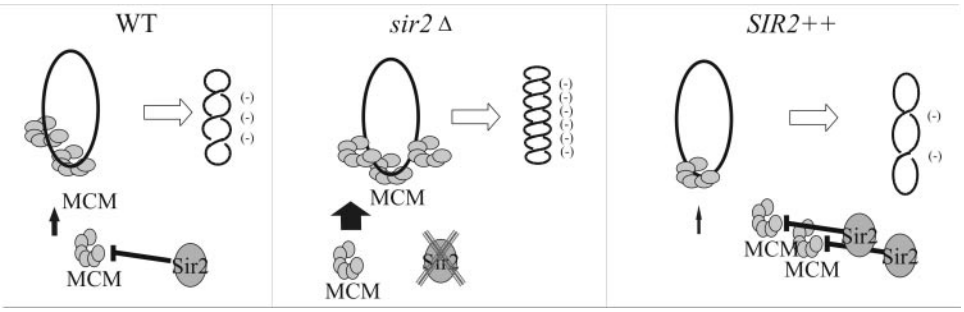

Figure 7. Interpretive model to account for the topological effect of the *sir2*Δ mutation. In WT cells, a defined amount of the MCM complex is bound to DNA, producing the observed level of supercoiling (equilibrium level). When Sir2p is absent, plasmid DNA is overloaded with the MCM complex, leading to increased negative supercoiling. In a strain overexpressing Sir2p, the excess protein limits loading of the MCM complex, leading to positive supercoiling.

topoisomerase I would act to relax this torsional stress, yielding a more negatively supercoiled DNA. Likewise, less efficient loading of the MCM complex on plasmids could be the cause of positive supercoiling. To test this hypothesis, we analyzed the *mcm7-td* mutant for topoisomer distribution (Figure 6). Actually, under inducing conditions (galactose), a more positively supercoiled distribution of topoisomers than expected is evident.

Thus, the overall conclusion is that Sir2p limits MCM complex loading onto ARSs: in the *sir2*Δ mutant, overloading of the complex increases the unwinding of DNA, leading to negative supercoiling of plasmids (see model in Figure 7). Based on our demonstration that the only amino acid hyperacetylated in plasmid chromatin is H4-K16, we hypothesize that a specific histone deacetylase activity is involved in the reported phenotypes, and more specifically that H4-K16 hyperacetylation represents a signal for the recruitment of additional factor(s), such as the MCM complex. This is in agreement with previous data (18) showing that loss of Sir2p catalytic activity increases MCM loading on ARS sequences. We cannot eliminate the possibility that our results were due not only to the Sir2p histone-deacetylase activity on H4-K16, but also to its putative ability to deacetylate different proteins. In fact, Sir2p homologues in other species, including mammals, have been demonstrated to deacetylate non-histone proteins as well (60). A further interpretation of our data are that it might reflect direct deacetylation activity of Sir2p on the MCM complex, with the consequent alteration of its function in the assembly of the Pre-RC complex. In support of this hypothesis, it has been demonstrated that Mcm3p is acetylated in mammalian cells (61).

Our demonstration that the topology of plasmids is altered in *sir2*Δ mutants reveals a new phenotype for this gene; whether the effect is directly mediated by the MCM complex or follows indirect pathways will be the subject of future investigations.

Note

During the reviewing process one of the anonymous reviewers suggested the following interpretation in order to explain our observation that larger plasmids were less responsive in our assays than the smaller ones.

The explanation suggested is that the positive superhelicity induced by a given amount of MCM-mediated strand separation would be distributed over a greater number of bp in the larger plasmids, resulting in lower topological strain (1100RT/bp)($L-L_0$). Lower strain would result in less distortion in twist along the molecule, which is the actual target of topisomerase (particularly type I) activity, and thus a smaller *in vivo* change in linking number. The authors are thankful to the reviewer and agree with this interpretation.

ACKNOWLEDGEMENTS

This work was partially supported by the ≪Istituto Pasteur-Fondazione Cenci Bolognetti≫ Universita' di Roma ≪La Sapienza≫. The authors are thankful to J. Broach for providing the Y1422 (*sir2*Δ) strain and the pAR44 plasmid; to D. Moazed for providing the *net1*Δ; to M. Grunstein for STY30 (*sir2*Δ), STY36 (*sir4*Δ) and *LJY912 (K16Q)* strains; J. F. Diffley for *mcm7-td* strain and A. E. Ehrenhofer-Murray for providing the AEY1956 (K16R) strain. The authors also acknowledge F. Cioci, L. Fabiani and M. Caserta for critical reading of the manuscript. The authors are especially grateful to Dr J. A. Wise for helping us in editing the manuscript. Funding to pay the Open Access publication charges for this article was provided by GPA 2005, Università di Roma La Sapienza.

Conflict of interest statement. None declared.

REFERENCES

1. Gasser,S.M. and Cockell,M.M. (2001) The molecular biology of the SIR proteins. *Gene*, **279**, 1–16.
2. Imai,S., Armstrong,C.M., Kaeberlein,M. and Guarente,L. (2000) Transcriptional silencing and longevity protein Sir2 is an NAD-dependent histone deacetylase. *Nature*, **403**, 795–800.
3. Landry,J., Sutton,A., Tafrov,S.T., Heller,R.C., Stebbins,J., Pillus,L. and Sternglanz,R. (2000) The silencing protein SIR2 and its homologs are NAD-dependent protein deacetylases. *Proc. Natl Acad. Sci. USA*, **97**, 5807–5811.
4. Smith,J.S., Brachmann,C.B., Celic,I., Kenna,M.A., Muhammad,S., Starai,V.J., Avalos,J.L., Escalante-Semerena,J.C., Grubmeyer,C., Wolberger,C. *et al*. (2000) A phylogenetically conserved NAD+-dependent protein deacetylase activity in the Sir2 protein family. *Proc. Natl Acad. Sci. USA*, **97**, 6658–6663.
5. Frye,R.A. (1999) Characterization of five human cDNAs with homology to the yeast SIR2 gene: Sir2-like proteins (sirtuins) metabolize NAD and may have protein ADP-ribosyltransferase activity. *Biochem Biophys Res Commun.*, **260**, 273–279.
6. Tanner,K.G., Landry,J., Sternglanz,R. and Denu,J.M. (2000) Silent information regulator 2 family of NAD- dependent histone/protein deacetylases generates a unique product, 1-O-acetyl-ADP-ribose. *Proc. Natl Acad. Sci. USA*, **97**, 14178–14182.

7. Brachmann,C.B., Sherman,J.M., Devine,S.E., Cameron,E.E., Pillus,L. and Boeke,J.D. (1995) The SIR2 gene family, conserved from bacteria to humans, functions in silencing, cell cycle progression, and chromosome stability. *Genes Dev*., **9**, 2888–2902.
8. Blander,G. and Guarente,L. (2004) The Sir2 family of protein deacetylases. *Annu. Rev. Biochem*., **73**, 417–435.
9. Derbyshire,M.K., Weinstock,K.G. and Strathern,J.N. (1996) HST1, a new member of the SIR2 family of genes. *Yeast*, **12**, 631–640.
10. Rine,J. and Herskowitz,I. (1987) Four genes responsible for a position effect on expression from HML and HMR in *Saccharomyces cerevisiae*. *Genetics*, **116**, 9–22.
11. Shou,W., Seol,J.H., Shevchenko,A., Baskerville,C., Moazed,D., Chen,Z.W., Jang,J., Shevchenko,A., Charbonneau,H. and Deshaies,R.J. (1999) Exit from mitosis is triggered by Tem1-dependent release of the protein phosphatase Cdc14 from nucleolar RENT complex. *Cell*, **97**, 233–244.
12. Straight,A.F., Shou,W., Dowd,G.J., Turck,C.W., Deshaies,R.J., Johnson,A.J. and Moazed,D. (1999) Net1, a Sir2-associated nucleolar protein required for rDNA silencing and nucleolar integrity. *Cell*, **97**, 245–256.
13. Fritze,C.E., Verschueren,K., Strich,R. and Esposito,R.E. (1997) Direct evidence for SIR2 modulation of chromatin structure in yeast rDNA. *EMBO J*., **16**, 6495–6509.
14. Cioci,F., Vogelauer,M. and Camilloni,G. (2002) Acetylation and accessibility of rDNA chromatin in *Saccharomyces cerevisiae* in (Delta)top1 and (Delta)sir2 mutants. *J. Mol. Biol*., **322**, 41–52.
15. Gottlieb,S. and Esposito,R.E. (1989) A new role for a yeast transcriptional silencer gene, SIR2, in regulation of recombination in ribosomal DNA. *Cell*, **56**, 771–776.
16. Sinclair,D.A. and Guarente,L. (1997) Extrachromosomal rDNA circles--a cause of aging in yeast. *Cell*, **91**, 1033–1042.
17. Pasero,P., Bensimon,A. and Schwob,E. (2002) Single-molecule analysis reveals clustering and epigenetic regulation of replication origins at the yeast rDNA locus. *Genes Dev*., **16**, 2479–2484.
18. Pappas,D.L., Jr, Frisch,R. and Weinreich,M. (2004) The NAD(+)-d ependent Sir2p histone deacetylase is a negative regulator of chromosomal DNA replication. *Genes Dev*., **18**, 769–781.
19. Christman,M.F., Dietrich,F.S. and Fink,G.R. (1988) Mitotic recombination in the rDNA of *S. cerevisiae* is suppressed by the combined action of DNA topoisomerases I and II. *Cell*, **55**, 413–425.
20. Bryk,M., Banerjee,M., Murphy,M., Knudsen,K.E., Garfinkel,D.J. and Curcio,M.J. (1997) Transcriptional silencing of Ty1 elements in the RDN1 locus of yeast. *Genes Dev*., **11**, 255–269.
21. Smith,J.S. and Boeke,J.D. (1997) An unusual form of transcriptional silencing in yeast ribosomal DNA. *Genes Dev*., **11**, 241–254.
22. Robyr,D., Suka,Y., Xenarios,I., Kurdistani,S.K., Wang,A., Suka,N. and Grunstein,M. (2002) Microarray deacetylation maps determine genome-wide functions for yeast histone deacetylases. *Cell*, **109**, 437–446.
23. Germond,J.E., Hirt,B., Oudet,P., Gross-Belard,M. and Chambon,P. (1975) Folding of the DNA double helix in chromatin-like structures from simian virus 40 DNA. *Proc. Natl Acad. Sci. USA*, **72**, 1842–1847.
24. Shure,M. and Vinograd,J. (1976) The number of superhelical turns in native virion SV40 DNA and Minicol DNA determined by the band counting method. *Cell*, **8**, 215–226.
25. Simpson,R.T., Thoma,F. and Brubaker,J.M. (1985) Chromatin reconstituted from tandemly repeated cloned DNA fragments and core histones: a model system for study of higher order structure. *Cell*, **42**, 799–808.
26. Abraham,J., Feldman,J., Nasmyth,K.A., Strathern,J.N., Klar,A.J.S., Broach,J.R. and Hicks,J.B. (1982) Sites required for position-effect regulation of mating type information in yeast. *Cold Spring Harbor Symp. Quant. Biol*., **47**, 989–998.
27. Foss,M. and Rine,J. (1993) Molecular definition of the PAS1-1 mutation which affects silencing in *Saccharomyces cerevisiae*. *Genetics*, **135**, 931–935.
28. Bi,X. and Broach,J.R. (1997) DNA in transcriptionally silent chromatin assumes a distinct topology that is sensitive to cell cycle progression. *Mol. Cell. Biol*., **17**, 7077–7087.
29. Ansari,A. and Gartenberg,M.R. (1997) The yeast silent information regulator Sir4p anchors and partitions plasmids. *Mol. Cell. Biol*., **17**, 7061–7068.
30. Norton,V.G., Imai,B.S., Yau,P. and Bradbury,E.M. (1989) Histone acetylation reduces nucleosome core particle linking number change. *Cell*, **57**, 449–457.
31. Bauer,W.R., Hayes,J.J., White,J.H. and Wolffe,A.P. (1994) Nucleosome structural changes due to acetylation. *J. Mol. Biol*., **236**, 685–690.
32. Vogelauer,M., Cioci,F. and Camilloni,G. (1998) DNA protein–interactions at the *Saccharomyces cerevisiae* 35 S rRNA promoter and in its surrounding region. *J. Mol. Biol*., **275**, 197–209.
33. Liu,H., Krizek,J. and Bretscher,A. (1992) Construction of a GAL1-regulated yeast cDNA expression library and its application to the identification of genes whose overexpression causes lethality in yeast. *Genetics*, **132**, 665–673.
34. Mumberg,D., Müller,R. and Funk,M. (1994) Regulatable promoters of *Saccharomyces cerevisiae*: comparison of transcriptional activity and their use for heterologous expression. *Nucleic Acids Res*., **22**, 5767–5768.
35. Mumberg,D., Muller,R. and Funk,M. (1995) Yeast vectors for the controlled expression of heterologous proteins in different genetic backgrounds. *Gene*, **156**, 119–122.
36. Rose,M.D., Novick,P., Thomas,J.H., Botstein,D. and Fink,G.R. (1987) A *Saccharomyces cerevisiae* genomic plasmid bank based on a centromere-containing shuttle vector. *Gene*, **60**, 237–243.
37. Holmes,S.G., Rose,A.B., Steuerle,K., Saez,E., Sayegh,S., Lee,Y.M. and Broach,J.R. (1997) Hyperactivation of the silencing proteins, Sir2p and Sir3p, causes chromosome loss. *Genetics*, **145**, 605–614.
38. Lianna,M.J., Kayne,P.S., Kahn,E.S. and Grunstein,M. (1990) Genetic evidence for an interaction between SIR3 and histone H4 in the repression of the silent mating loci in *Saccharomyces cerevisiae*. *Proc. Natl Acad. Sci. USA*, **87**, 6286–6290.
39. Sherman,F., Fink,G.R. and Lawrence,C. (1983) *Methods in Yeast Genetics*. Cold Spring Harbor University Press, Cold Spring Harbor.
40. Longtine,M.S., McKenzie,A., III, Demarini,D.J., Shah,N.G., Wach,A., Brachat,A., Philippsen,P. and Pringle,J.R. (1998) Additional modules for versatile and economical PCR-based gene deletion and modification in *Saccharomyces cerevisiae*. *Yeast*, **14**, 953–961.
41. Venditti,S. and Camilloni,G. (1994) *In vivo* analysis of chromatin following nystatin-mediated import of active enzymes into *Saccharomyces cerevisiae*. *Mol. Gen. Genet*., **242**, 100–104.
42. Di Mauro,E., Camilloni,G., Verdone,L. and Caserta,M. (1993) DNA topoisomerase I controls the kinetics of promoter activation and DNA topology in *Saccharomyces cerevisiae*. *Mol. Cell. Biol*., **13**, 6702–6710.
43. Peck,L.J. and Wang,J.C. (1983) Energetics of B-to-Z transition in DNA. *Proc. Natl Acad. Sci. USA*, **80**, 6206–6210.
44. Hecht,A., Strahl-Bolsinger,S. and Grunstein,M. (1995) Spreading of transcriptional repressor SIR3 from telomeric heterochromatin. *Nature*, **383**, 92–96.
45. Hecht,A. and Grunstein,M. (1999) Mapping DNA interaction sites of chromosomal proteins using immunoprecipitation and polymerase chain reaction. *Meth. Enzymol*., **304**, 399–414.
46. Huang,J. and Moazed,D. (2003) Association of the RENT complex with nontranscribed and coding regions of rDNA and a regional requirement for the replication fork block protein Fob1 in rDNA silencing. *Genes Dev*., **17**, 2162–2176.
47. Liu,L.F. and Wang,J.C. (1987) Supercoiling of the DNA template during transcription. *Proc. Natl Acad. Sci. USA*, **84**, 7024–7027.
48. Sikorski,R.S. and Hieter,P. (1989) A system of shuttle vectors and yeast host strains designed for efficient manipulation of DNA in *Saccharomyces cerevisiae*. *Genetics*, **122**, 19–27.
49. Bach,M.L., Lacroute,F. and Botstein,D. (1979) Evidence for transcriptional regulation of orotidine-5′-phosphate decarboxylase in yeast by hybridization of mRNA to the yeast structural gene cloned in *Escherichia coli*. *Proc. Natl Acad. Sci. USA*, **76**, 386–390.
50. Braunstein,M., Rose,A.B., Holmes,S.G., Allis,C.D. and Broach,J.R. (1993) Transcriptional silencing in yeast is associated with reduced nucleosome acetylation. *Genes Dev*., **7**, 592–604.
51. Strahl-Bolsinger,S., Hecht,A., Luo,K. and Grunstein,M. (1997) SIR2 and SIR4 interactions differ in core and extended telomeric heterochromatin in yeast. *Genes Dev*., **11**, 83–93.
52. Ghidelli,S., Donze,D., Dhillon,N. and Kamakaka,R.T. (2001) Sir2p exists in two nucleosome-binding complexes with distinct deacetylase activities. *EMBO J*., **20**, 4522–4535.
53. Tanny,J.C., Kirkpatrick,D.S., Gerber,S.A., Gygi,S.P. and Moazed,D. (2004) Budding yeast silencing complexes and regulation of Sir2 activity by protein–protein interactions. *Mol. Cell. Biol*., **24**, 6931–6946.

54. Braunstein,M., Sobel,R.E., Allis,C.D., Turner,B.M. and Broach,J.R. (1996) Efficient transcriptional silencing in *Saccharomyces cerevisiae* requires a heterochromatin histone acetylation pattern. *Mol. Cell. Biol.*, **16**, 4349–4356.
55. Labib,K., Tersero,J.A. and Diffley,J.F. (2000) Uninterrupted MCM2-7 function required for DNA replication fork progression. *Science*, **288**, 1643–1647.
56. Broach,J.R., Li,Y.Y., Feldman,J., Jayaram,M., Abraham,J., Nasmyth,K.A. and Hicks,J.B. (1982) Localization and sequence analysis of yeast origins of DNA replication. *Cold Spring Harbor Symp. Quant. Biol.*, **47**, 1165–1173.
57. Van Houten,J.V. and Newlon,C.S. (1990) Mutational analysis of the consensus sequence of a replication origin from yeast chromosome III. *Mol. Cell. Biol.*, **10**, 3917–3925.
58. Hoppe,G.J., Tanny,J.C., Rudner,A.D., Gerber,S.A., Danaie,S., Gygi,S.P. and Moazed,D. (2002) Steps in assembly of silent chromatin in yeast: Sir3-independent binding of a Sir2/Sir4 complex to silencers and role for Sir2-dependent deacetylation. *Mol. Cell. Biol.*, **22**, 4167–4180.
59. Forsburg,S.L. (2004) Eukaryotic MCM proteins: beyond replication initiation. *Microbiol. Mol. Biol. Rev.*, **68**, 109–131.
60. Vaziri,H., Dessain,S.K., Ng Eaton,E., Imai,S.I., Frye,R.A., Pandita,T.K., Guarente,L. and Weinberg,R.A. (2001) hSIR2(SIRT1) functions as an NAD-dependent p53 deacetylase. *Cell*, **107**, 149–159.
61. Takei,Y., Swietlik,M., Tanoue,A., Tsujimoto,G., Kouzarides,T. and Laskey,R. (2001) MCM3AP, a novel acetyltransferase that acetylates replication protein MCM3. *EMBO Rep.*, **2**, 119–123.